MELiSSA

TECHNICAL NOTE

Memorandum of Understanding TOS-MCT/2002/3161/In/CL

TECHNICAL NOTE: 86.4.9

FINAL TECHNICAL NOTE

prepared by/*préparé par*	Tobias Albrecht, Gerd Brunner TU Hamburg-Harburg, Thermal Process Engineering
reference/*réference*	14719/00/NL/SH
issue/*édition*	1
revision/*révision*	0
date of issue/*date d'édition*	30/03/06
status/*état*	Draft
Document type/*type dedocument*	Technical Note
Distribution/*distribution*	

CONFIDENTIAL DOCUMENT

APPROVAL

Title *titre*	issue 1 *issue*	revision 0 *revision*

author *auteur*	date 30/03/06 *date*

approved by *approuvé by*	date *date*

CHANGE LOG

reason for change */raison du changement*	issue/*issue*	revision/*revision*	date/*date*

CHANGE RECORD

Issue: 1 Revision: 0

reason for change/*raison du changement*	page(s)/*page(s)*	paragraph(s)/*paragraph(s)*

Table Of Contents

1 INTRODUCTION

Plant biomass is the world's most abundant source of energy and can serve as a direct nourisher as well as a feedstock for chemical products. Therefore numerous attempts to effectively utilize biomass have been undertaken in the past. One of the most promising approaches in converting materials derived from biomass to useful products is the hydrothermal treatment, also known as hydrothermolysis, employing near- and supercritical water as a reaction medium [1]. Subjecting biomass to water near its critical state offers the potential of high degrees of conversion within short residence times, compared to alternative treatment methods like the biodegradation based on microorganisms. With respect to the product distribution, high selectivities can be achieved by adjusting the operating temperature and/or pressure, leading to changes in water density, the ionic product and the dielectric constant over a wide range of conditions and thus favoring different decomposition pathways. Due to these advantages, the hydrothermal treatment becomes especially attractive when a close to complete recycling of all of the components is required, as might be encountered in future, microorganism and higher plant based life support systems. In such applications, biomass offers the potential of an almost complete recycling of all of its components by harvesting and consuming its edible parts, followed by a sub- or supercritical water treatment of the wastes generated and the subsequent, renewed build-up of plant biomass, thus closing the cycle.

Due to the unique features of water near its critical point, the conversion of biomass derived materials in sub-and supercritical water can serve as a supplement or an alternative to biological degradation techniques. The main advantages of subjecting biomass to such a hydrothermal treatment, namely the conversion at high space-time-yields, become of especially high significance when a close to complete recycling of the biomass components is required. Against this background of a fast reutilization of biomass in such systems, the present work was part of a new phase of research and development on MELISSA (Micro-Ecological Life Support System Alternative) conceived by the European Space Agency (ESA). MELISSA constitutes a self contained ecosystem based on micro-organisms and higher plants and is intended as a tool to gain knowledge and understanding about the behavior of artificial ecosystems. If the design of such an artificial ecosystem proves to be feasible and if the test results are satisfactory with respect to the requirements imposed on the project, it is planned to apply this knowledge to the development of a biological life support system in the long-term perspective. In the following the scheme of the MELISSA project thus far is explained in order to get an insight into the main working principles and the problems associated with the current setup. The special needs and requirements of a biological life support system for long-duration manned space missions are also addressed.

In order for long-duration manned space missions, e.g. a lunar base or a mission to Mars, to become possible, a feasible life support system has to be designed. Special emphasis has to be placed on the treatment of waste streams including air purification and the treatment of both

aqueous and solid wastes. This need arises from the problem of limitations of resources as well as from hygienic demands. Therefore a life support system has not only to be capable of guaranteeing hygiene by purifying the waste streams, but it has also to be capable of achieving a high recycling rate of valuable components by degrading the wastes to useful products at a high rate of conversion.

The approach taken by MELISSA is to develop a concept involving the use of a small-scale artificial ecosystem. The main building blocks and the resulting fluxes are depicted schematically in Figure 1.1.

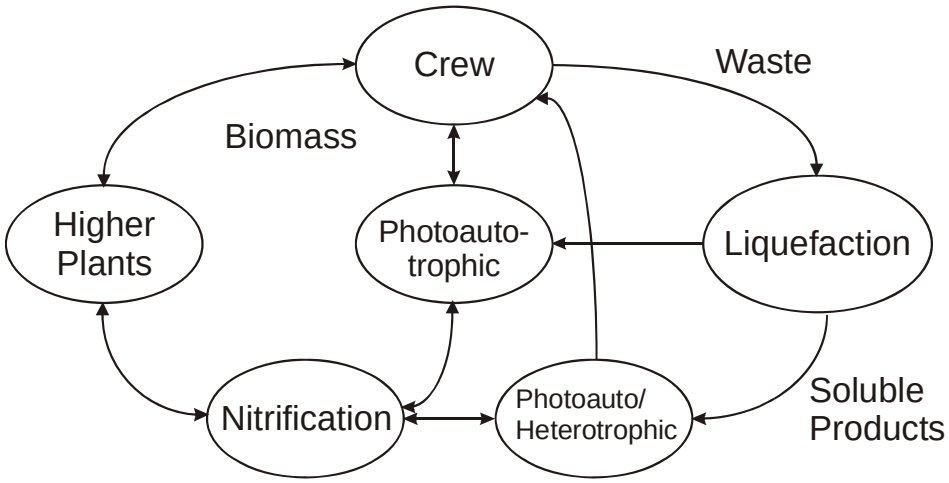

Figure 1.1: Current scheme of the artificial ecosystem of the MELISSA project

The Liquefaction, Nitrification and the Phototrophic biomass production constitute the major compartments of MELISSA. The Liquefaction compartment in the MELISSA loop is responsible for the biodegradation of wastes produced by the crew, e.g. fecal matters and urine as well as non-edible parts of plant material, paper and non-edible biomass. Subsequently, the effluent streams, composed mainly of the product gas carbon dioxide as well as fatty acids and ammonium, are subjected to the phototrophic compartments, e.g. the anaerobic photoauto/heterotrophic compartment II and the photoautotrophic compartment IV. Ammonium produced during the biodegradation of the aqueous and solid wastes is fed to the nitrifying compartment III, where it is oxidized to yield nitrate which in turn can be utilized in the photoautotrophic compartment IV and the higher plant compartment. The higher plant compartment was introduced into the MELISSA cycle to account for the crew's demand for a balanced diet. Higher plants under consideration in this approach include lettuce, wheat, potato, tomato, soybean, rice, spinach, and onion, whose edible parts are consumed by the crew. The inedible fraction of these higher plants, including leaves, roots and stems has to be degraded together with hygienic wastes and fecal matter, by which the overall cycle is closed.

However, the overall performance of the MELISSA cycle is hampered by the liquefying compartment, the part addressed in this project. Due to the particulate structure of plant material and fecal matter, the bacterial strains employed in the liquefaction so far have not proven to be capable of converting the particulate matter at a sufficiently high conversion rate within an acceptable residence time. Indeed, the microorganisms used in the biodegradation are optimally equipped to handle soluble molecules which leads to critical limitations in case that water insoluble substances are involved. The effect of the solubilisation being the rate-controlling step is particularly severe when fibrous components, which make up the major part of the inedible plant material, are subjected to the biological degradation process. Currently, an overall degradation efficiency of 60-65% is accomplished, the overall fibre degradation being about 75% [2].

There are several possible approaches to enhance the conversion of fibrous materials. One thinkable method is the chemical treatment of the wastes by adding certain reagents like Fenton's reagent, Schweizer's reagent or by adjusting the pH such that the acid catalyzed hydrolysis of cellulosic compounds is promoted. Such methods suffer the major drawback that additional treatment steps, e.g. neutralization and precipitation, may become unavoidable in the further processing of the waste water.

The most promising method is the thermal treatment of fibrous materials at elevated temperatures and pressures using water as a solvent. Water near and above its critical point (T_c = 647 K; p_c = 22.1 MPa) serves as an excellent reaction medium due to the high temperature and the increase in the ionic product and a change in the dielectric constant. As a result, compounds which are hardly soluble under ambient conditions can be dissolved to a high degree in water near its critical state. Due to the increased ionic product, water itself acts as an acid leading to an increase in the rate of hydrolysis and consequently to a high degree of decomposition. Since the fluid properties of water near the critical point can be varied over a wide range of conditions the effluent product distribution can possibly be controlled by adjusting operating temperature and/or pressure. Furthermore, the high temperature treatment provides an additional hygienic barrier against hazardous contaminants like pathogens.

The hydrothermal treatment suggested above was initially considered to be embedded in a multi-step biological solubilisation as depicted Figure 1.2.

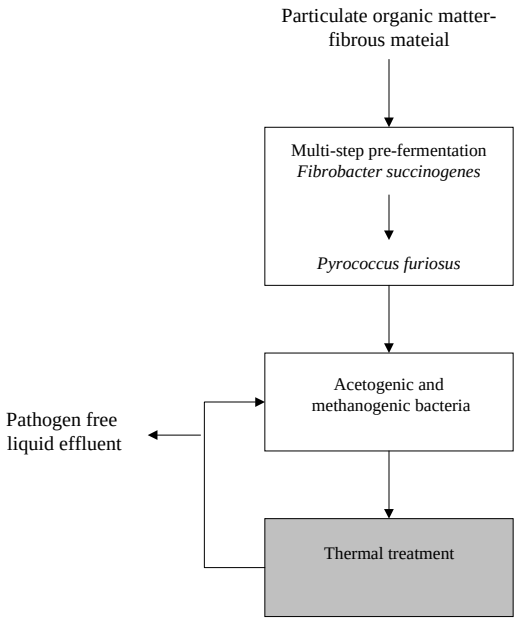

Figure 1.2: Initial scheme of the MAP project

According to the initially proposed scheme the particulate organic matter is subjected to a multi-step pre-fermentation involving Fibrobacter succinogenes, a strictly anaerobic bacterium, and Pyrococcus furiosus, an extremophilic organism growing at temperatures as high as 100°C. These processes can be applied in sequence and it is expected to thereby achieve a high rate of hydrolysis. Subsequently the soluble products are fed to a conventional anaerobic biogas digestion involving acetogenic and methanogenic bacteria. The gaseous products which are mainly composed of hydrogen and methane, can be separated from the liquid phase and can be supplied to the production of microbial protein, the so-called single cell protein or SCP. In the course of the project, the sequence of treatment steps was modified, meaning that the methanogenic reactor became the primary degradation step followed by the Fibrobacter and hydrothermal treatment.

The thermal treatment unit is considered to be implemented in succession to the anaerobic digestion compartment in the frame of the MAP project. By applying the high temperature and high pressure method as an after-treatment it is intended to not only remove any remaining insoluble matter within a short residence time in the order of minutes but also to guarantee an absolutely pathogen free effluent. Extra solubles obtained in the hydrothermal treatment are to be recycled to the anaerobic digestion compartment and subjected to biological degradation in the frame of this MAP-loop.

2 FUNDAMENTALS AND STATE OF KNOWLEDGE

2.1 Sub- and supercritical water

For a pure component, the supercritical state is defined as the state of a fluid above its critical temperature T_c and critical pressure p_c. [3]. The critical point marks the end point of the vapor pressure curve, such that there is no two-phase region but a one-phase supercritical region at conditions above the respective critical values. The supercritical region is denoted as the hatched area in Figure 2.1, which depicts a schematic PT-diagram of a pure component.

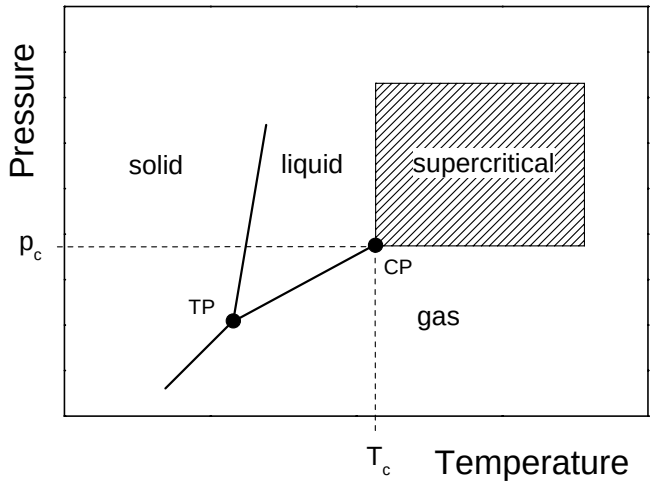

Figure 2.1: PT-diagram of a pure component [3], CP critical point, TP triple point

In many respects, the properties of a supercritical fluid lie in between those of a liquid and a gas. On the one hand the density of a supercritical fluid resembles that of a liquid, on the other hand supercritical fluids exhibit viscosities similar to those of gases. A compilation of important properties in the different states is depicted in Table 2.1.

Table 2.1: Properties of gases, liquids, and supercritical fluids [4]

	Gases	SCF (T_C, P_C)	SCF (T_C, $4P_C$)	Liquids
Density [kg/m^3]	0.6 - 2	200 - 500	400 -900	600 1600
Dynamic viscosity [Pa s]	$(1 – 3)\cdot10^{-5}$	$(1 – 3)\cdot10^{-5}$	$(3 – 9)\cdot10^{-5}$	$(0.2 – 3)\cdot10^{-3}$
Diffusion coefficient [m^2/s]	$(1 – 4)\cdot10^{-5}$	$7\cdot10^{-8}$	$2\cdot10^{-8}$	$(0.2 – 2)\cdot10^{-9}$

Due to the high densities, low viscosities, and the comparatively high diffusion coefficients, supercritical fluids exhibit excellent solvent and transport properties. Furthermore, the fluid properties can be continuously adjusted over a wide range by varying the conditions in terms of temperature and pressure. In the vicinity of the critical point, where the gradients in

physico-chemical properties are the largest, only small changes in temperature and pressure are required to significantly change properties. Supercritical fluids can thus be tuned over a broad range to optimise the properties with respect to the actual process.

Supercritical fluids have therefore been utilised in many applications. While in the past the focus was on extraction and fractionation processes, the use of supercritical fluids as reaction media has been gaining increasing attention during the last two decades. Both decomposition and synthesis reactions in supercritical fluids have been being studied [5, 6] with the objectives to optimise reaction conditions, replace conventional solvents, and allow for reaction pathways which are not feasible with alternative approaches.

Especially water at elevated temperatures and pressures offers many beneficial properties which make it an excellent solvent and reaction medium for a broad variety of applications [7, 8, 9, 10, 11]. Figure 2.2 shows a PT-diagram of water at elevated temperatures and pressures.

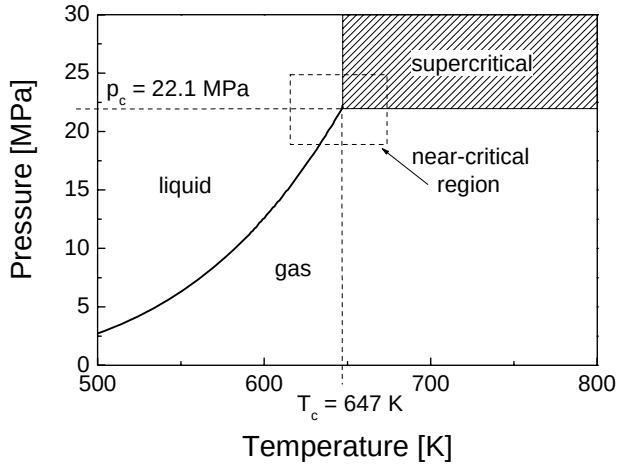

Figure 2.2: PT-diagram of water at elevated temperatures and pressures

Water has characteristically high critical values, which are T_c = 647 K and p_c = 22.1 MPa, respectively. With regard to nomenclature, one refers to “near-critical water” in the region which extends around the critical point, whereas the expression “subcritical water” denotes the non-supercritical, usually liquid state ($T<T_c$). There is, however, no precise definition as where the near-critical region is located. In general, the near-critical condition is referred to as the region in which high gradients in the physico-chemical properties of the substances are observed.

Sub- and supercritical water provides a thermally activated regime for fast kinetics. Besides, it shows a distinctly different behavior compared to water under ambient conditions, which is due to the dramatic changes in thermodynamic properties. One important property with respect

to the polarity of water is its dielectric constant [12, 13]. The dielectric constant ε as a function of temperature and density is depicted in Figure 2.3.

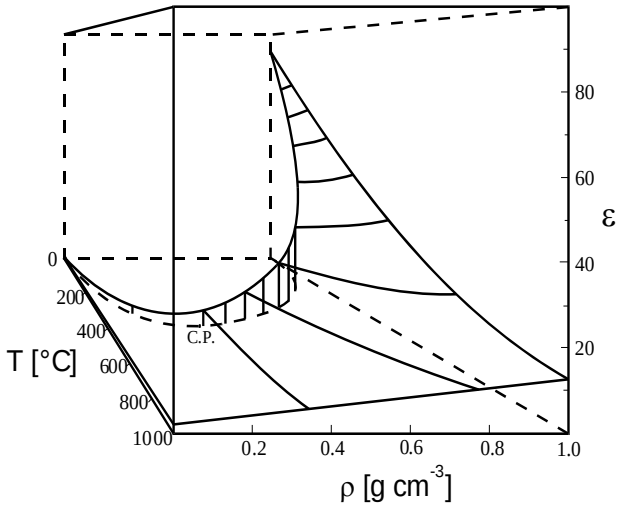

Figure 2.3: Dielectric constant of water [13]

As can be seen, the dielectric constant drops by an order of magnitude from a value of about 80 at ambient conditions, but water still remains a polar fluid. The significant drop in the dielectric strength leads to a much increased solvent power for most organic compounds, thus providing a homogeneous reaction atmosphere. In such cases no phase boundaries impose any mass transfer limitations on the reactions and more chemical bonds are accessible to reaction steps. Many works were therefore focused on the removal and destruction of organic pollutants with supercritical water [14, 15, 16, 17].
Dissociation of water leads to the formation of hydronium and hydroxyl ions and determines the pH of pure water. The ion product changes drastically from ambient to subcritical and supercritical conditions [18, 19] as illustrated in Figure 2.4.

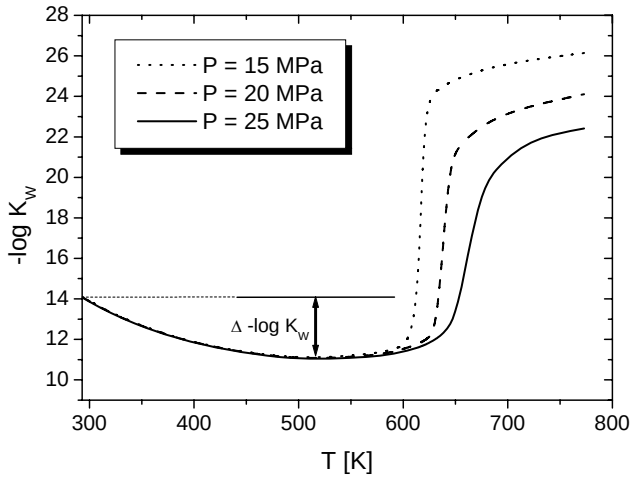

Figure 2.4: Ion product of water at elevated temperatures and pressures [18]

The ion product of water is represented by an empirical equation based on density and two quadratic functions of temperature.

$$\log K_W = A + B/T + C/T^2 + D/T^3 + (E + F/T + G/T^2)\log \rho_W \qquad (2.1)$$

where ρ_W denotes the density of pure water at given temperature and pressure. This equation serves as the background for the international formulation for the ion product of water. It was obtained by fitting several sets of experimental data and it is believed to represent the ion product of water for a temperature range from 0 to 1000°C and pressures ranging from 0.1 to 1,000 MPa.
Figure 2.4 shows that the ion product rises from a value of 10^{-14} at ambient conditions to values up to 10^{-11} in the subcritical region, corresponding to an increase by three orders of magnitude. Due to the associated increase in activity of hydronium- and hydroxyl ions, subcritical water itself promotes acid and base catalysed reactions without any additional catalysts like mineral acids. Accordingly, many ionic reactions, e.g. the hydrolysis of biopolymers, proceed at a maximum rate under subcritical conditions.
In this context, hydrolysis refers to the cleavage of bonds under the influence of water [20] according to the scheme illustrated in Figure 2.5.

$$A - B + H - OH \rightarrow A - H + B - OH$$

Figure 2.5: Formal scheme of the hydrolytic cleavage of bond A-B

Important hydrolysis reactions are the cleavage of glycosidic bonds of polysaccharides, e.g. starch and cellulose [21, 22], of polypeptides to yield protein hydrolyzates and free amino acids [23, 24, 25], as well as the hydrolysis of esters [26].
In contrast, the ion product drastically drops at near- and supercritical conditions as a result of the strong decrease in water density. In general, ionic reaction pathways are favoured at higher water densities, whereas the lower densities at supercritical conditions lead to free radical reaction mechanisms being the preferred reaction pathways [27, 28].
It can also be inferred that pressure does not have a noticeable influence on the ion product at temperatures below 300°C. This observation can be explained by the fact that water still has the character of an incompressible fluid at these conditions, meaning that pressure does not markedly affect density and hence the ion product.

Due to these unique features, near-critical water serves as an excellent reaction medium and is a highly attractive supplement or alternative to biological treatment methods, especially when hardly biodegradable substances like cellulose or related compounds are involved. Near-critical water offers the possibility of controlling and influencing the degradation product distribution by slightly adjusting the operating parameters in terms of pressure and temperature. The treatment in high-temperature water does not only offer the potential of complete conversion at high space-time yields, but it also serves a hygienic barrier, by which the sterility of effluents could be accomplished.
In contrast, the usage of sub- and supercritical water is only associated with limited problems. Salt deposition and corrosion of reactor material are counted among the general drawbacks of supercritical water processes. The precipitation and subsequent deposition of salts is due to the decreased solvent power for ionic species at supercritical conditions.

The degradation of biopolymers and destruction of pollutants can further be enhanced by supplementary means. The acidification by carbon dioxide leads to a decrease in pH, which favours acid catalysed steps like the hydrolysis of ester and ether bonds in biomolecules. The addition of an oxidant to high-temperature water is a very efficient technique to mineralise hydrocarbons by conversion to carbon dioxide, thus achieving a complete destruction of any organic material.

2.2 The system water/carbon dioxide

The pH of the aqueous phase in the system water-CO_2 decreases due to the increased solubility of carbon dioxide in water and the dissociation of carbonic acid according to the following scheme:

$$CO_2 + H_2O \leftrightarrow H_2CO_3 \leftrightarrow H^+ + HCO_3^-$$

Figure 2.6: Reaction scheme of carbonic acid dissociation in water

The acidification by carbon dioxide is assumed to result in a rate enhancement of acid-catalysed reaction steps without the need to add any mineral acids like hydrochloric acid. This approach offers the potential to easily recover carbon dioxide by expansion after treatment and to reuse it by recirculation as opposed to excessive neutralisation and precipitation steps, which become necessary when applying mineral acids.

Investigations on the use of carbon dioxide as a catalyst in water at elevated temperatures and pressures are scarce. Only a limited number of works have been published, e.g. the hydrolysis of starch [29], [30], and the dehydration of cyclohexanol and the alkylation of p-cresol [31]. Besides, water/carbon dioxide-mixtures were successfully employed in the remediation of soils contaminated with heavy metals [32], [33]. As a result of the drop in pH, the mobility of metal ions could be enhanced as compared to the treatment with pure water. The hydrolysis of lignocellulosic materials in water/carbon dioxide-mixtures has not been reported before.

A graphical representation of the pH of aqueous solutions saturated with carbon dioxide is given in [34]. Figure 2.7 shows the pH as a function of temperature for different pressures.

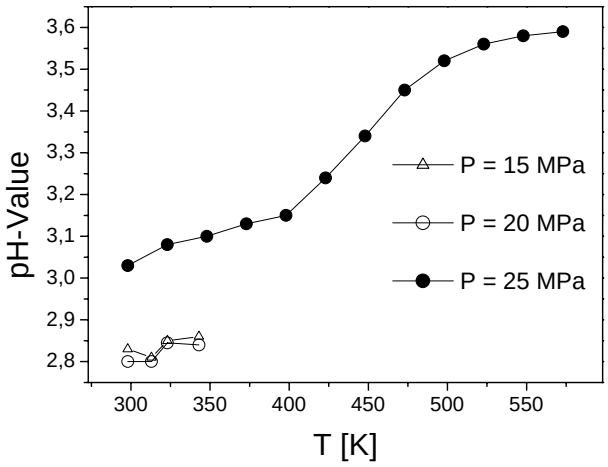

Figure 2.7: pH-value of high-temperature water saturated with carbon dioxide [34]

The values for a pressure of 25 MPa were calculated [32] on the basis of equilibrium data for the system water-CO_2 [35] and the first dissociation constant of carbonic acid [36]. The data depicted for pressures of 15 and 20 MPa were determined experimentally through direct measurement of the pH in a view cell by spectrophotometric methods [37]. The pH-value shows a decrease with increasing pressure and temperature. For the conditions applied in this work, the pH of water saturated with carbon dioxide is in the range of 3.6-3.7.

The pH as a function of the carbon dioxide concentration in the aqueous phase can be determined by solving the respective charge balance:

$$[H^+] = [OH^-] + [HCO_3^-] + 2[CO_3^{2-}] \qquad (2.2)$$

where the values stated in brackets denote the molal concentration of species. The last term on the right hand side, the concentration of bicarbonate, can be neglected because of the low value of the second dissociation constant of carbonic acid.

Both the dissociation of water and the dissociation of carbonic acid contribute to the concentration of hydronium ions according to the following equations:

$$K_W = [H^+][OH^-] \qquad (2.3)$$

$$K_1 = [H^+][HCO_3^-]/[CO_{2,aq}] \qquad (2.4)$$

Isolation for the concentration of hydroxyl ions and carbonate ions, respectively, and substitution into equation 2.2 yields

$$[H^+] = K_W/[H^+] + K_1[CO_{2,aq}]/[H^+] \qquad (2.5)$$

from which the concentration of hydronium ions and the associated pH of the system can be calculated.

Figure 2.8 shows the pH of water/carbon dioxide-mixtures as a function of carbon dioxide concentration.

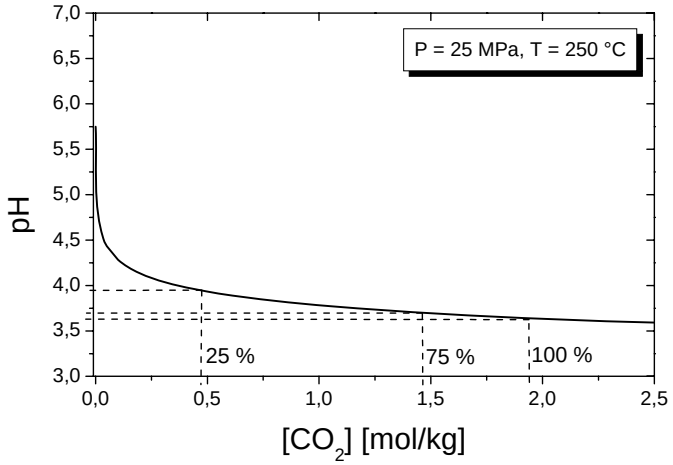

Figure 2.8: pH of water as a function of CO_2-concentration, the percent values are stated with respect to the saturation concentration

The pH decreases by two orders of magnitude up to the saturation level as compared to pure water at the same conditions. Due to the logarithmic character of the underlying equation, the pH initially drops sharply and lowers progressively slower with increasing carbon dioxide addition. Accordingly, addition of carbon dioxide beyond a degree of saturation of 75 % does not significantly contribute to a further decrease in pH and associated rate enhancement of acid catalysed reaction steps.

3 EXPERIMENTAL METHODS

In this work, model compounds, e.g. pure cellulose and lignin, as well as real lignocellulosic wastes were treated in sub- and supercritical water. The experiments were conducted in fully-continuous mode in a tubular reactor at both hydrolytic and oxidative conditions, covering a wide temperature range from 200 to 500°C, residence times in the order of a few seconds up to three minutes, and pressures up to 30 MPa. Because of the continuous processing of particulate matter at flow rates lower than 5 kg/h, the initial biomass concentrations were limited to a maximum of two percent by weight. At higher initial solid concentrations, the narrow architecture of the pump head and the fibrous structure of the solids led to problems due to clogging. The acidification by carbon dioxide as an alternative means to enhance the rate of hydrolysis was also studied. In addition to the fully continuous mode of operation, semi-continuous experiments were performed. In order to increase the residence time of biomass in the reactor, the solid material was retained in a fixed bed set-up and treated by a continuous flow of sub- and supercritical water.

The materials and the experimental set-up used in this work are presented in the following. The analytical methods for the characterization of the input material and the effluents are also discussed.

3.1 Materials

For the experiments on model compound studies, pure cellulose and lignin were employed. Micro-crystalline cellulose (Avicel) with a purity of 99 % was purchased from Merck. Water-insoluble organosolv lignin from the treatment of hardwoods (M_W = 3500 g/mol) and alkali lignin (M_W = 28000 g/mol) were purchased from Sigma-Aldrich. These materials were obtained as a fine powder and could be used as received without additional pre-treatment at initial solid concentrations of up to one wt-%. The suspensions were prepared by weighing the amount of material with a laboratory scale and adding the respective amount of demineralized water. For the experimental studies on the biosafety of effluents, bovine serum albumin and naphthalene were purchased from Merck and were used as received.

Wheat straw was provided by a local farmer. It was first ground in a cutting mill (IKA, MF10 Basic) to particle sizes of less than 250 µm. The obtained powder was subsequently treated in a coffee mill for further size reduction. Particles passing a sieve with a mesh size of 112 µm were used for preparing the suspension.

The composition of the model waste specified by ESA is stated in Table 3.1.

Table 3.1: Composition of model waste and respective suppliers

Component	Portion [wt-%]	Source	DM content [wt-%]
Wheat straw	23.3	Local farmer	94.5
Cabbage	23.3	Market	9.7
Soya	23.3	Oil-mill	91.1
Algae	10	BlueBioTechGmbH	95.5
Faecal material	20	-	27.4

The dry matter content of faecal material was not determined experimentally but calculated from literature data [38]. The composition depicted in the table was based on the original idea of ESA to treat a waste which was as close to reality as possible. Due to hygienic concerns, the faecal material was omitted and the other substrate ingredients were adjusted according to their ratios as specified by ESA.

The preparation of the model waste specified by ESA consisted of a multi-step size reduction procedure in order to obtain sufficiently fine particles that could be handled continuously in the flow reactor. Wheat straw and soya were prepared by dry size reduction methods with a rotary cutter and a conventional coffee mill. This approach was not feasible for the cabbage because of the high water content. The cabbage was first treated with a knife and a grater. The resulting pulp was subsequently subjected to a kitchen mixer with the addition of extra water. The cabbage was finally homogenized by an Ultra-TORAX (Heidolph DIAX 900) together with the algae, which did not require any additional treatment prior to homogenisation.

Digester residues from Partner 1 were received in the form of dry agglomerates or sludge. In the case of agglomerates, the residues were directly treated by dry size reduction, while the sludge was first dewatered by vacuum filtration and subsequent overnight storage in a vacuum dryer.

Hydrogen peroxide was purchased from Merck as an aqueous solution with a concentration of 30 wt-%. It was stored in a cabinet and it was not introduced into the feed vessel until immediately before the start of experiment to avoid decomposition reactions. Carbon dioxide with a purity of 99.95 % (KWD) was taken from the gas phase of the central storage tank of the Institute at a pressure of 6 MPa.

3.2 Experimental set-up

3.2.1 SET-UP OF THE CONTINUOUS REACTION UNIT

A schematic sketch of the tubular reactor for the continuous treatment of lignocellulosic biomass is shown in Figure 3.1.

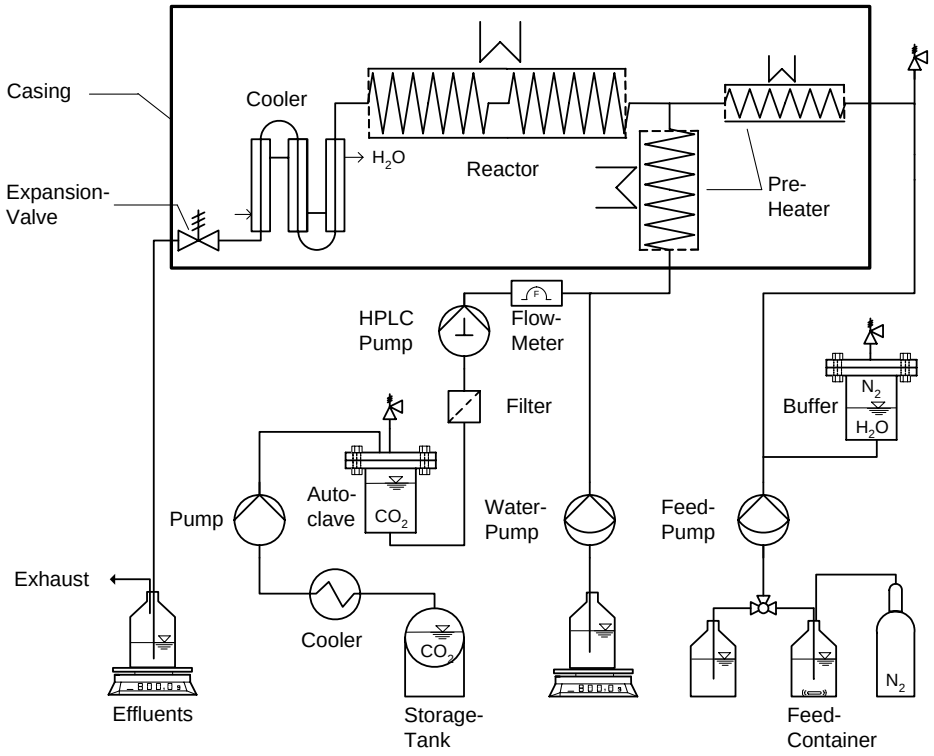

Figure 3.1:Schematic sketch of the experimental apparatus for the continuous treatment of biomass

The main building blocks of the apparatus were the supply lines for the biomass suspension, hot water, and carbon dioxide, the pre-heaters, the tubular reactor, and the downstream processing units, which consisted of the cooler, expansion valve, and the effluent collection system, respectively. The high pressure reaction unit was designed as a tubular reactor made of high temperature/pressure resistant steel (1.4404, OD = 6.35 mm, ID = 3.05 mm). The volume of the tubular reactor could be adjusted by installing coiled high pressure piping of different length. With the coils used in the experiments, which had internal volumes of 8 ml, 50 ml, and 100 ml, residence times in the order of a few seconds up to three minutes could be covered, depending on fluid density and mass flow rates. The flow reactor was capable of withstanding operating pressures up to 30 MPa and temperatures up to 400-450°C.

The feed suspension was fed from a 2 l closed glass flask covered with a plastic layer. The feed was agitated through a magnetic stirrer to prevent the particulate matter from settling and to ensure a homogeneous feed suspension throughout the vessel. In order to secure that no oxygen dissolved in the water and to study the hydrolytic and oxidative treatment separately, the feed suspension was put under a nitrogen atmosphere. This was accomplished by slightly pressurizing the flask with nitrogen gas, which was delivered from a compressed gas cylinder. The water storage tank contained pure demineralized water and served as the water supply until the desired operating conditions were reached and the system worked at steady state conditions in terms of temperature, pressure, and flow rate. The feed suspension was then pumped into the reactor by adjusting the position of a three-way valve in the suction line.

The feed suspension containing the particulate matter was introduced into the system by means of a high pressure membrane pump equipped with double ball valves at the suction and the discharge side (LEWA EK1/V metering pump). This redundant double ball configuration served the purpose of ensuring a reliable operation of the pump even if particles got trapped between one of the balls and its respective seat. In such a case, the second ball-seat pair was intended to secure the closure of the valve. Despite this configuration, it was not possible to reliably process particles larger than 200 µm at flow rates in the order of a few liters per hour. Especially the continuous delivery of real biomass, e.g. wheat straw and complex wastes, led to problems due to the fibrous structure of the material. In general, particles sizes of less than 112 to 180 µm and initial solid concentrations of 0.5 to maximal 2 wt-% were applied and could be satisfactorily processed by the feed pump. Although according to the manufacturer the membrane pump was supposed to exhibit a pressure firm characteristic, the system pressure revealed a noticeable influence on the metered flow rate. At an operating pressure of 25 MPa the maximum flow rate was in the range of 4 l/h.

Before entering the reaction unit the feed suspension was moderately pre-heated in an upstream coil, which had an inner volume of 38 ml and was made of the same piping material as the reactor. The power supply was accomplished by a 0.8 kW electric heating jacket. Typically, the feed suspension was heated up to a maximum temperature of 180-200°C in order to avoid the onset of decomposition reactions in the pre-heater.

In order to obtain meaningful results with respect to the residence time in the reactor at constant temperature conditions, the feed suspension had to be rapidly heated up to operating temperature. For this purpose, pure water was delivered to the apparatus with an additional high pressure metering pump (LEWA EL1) and heated up in two heating coils (45 ml, 2 kW each) to temperatures higher than the desired reaction temperature. Subsequently, this high water stream was mixed with the feed suspension through a mixing-tee at the inlet of the reactor. By this means, the temperature of the influent suspension could be instantaneously raised to the desired level and the temperature gradients along the reactor could be minimized, yielding close to isothermal conditions in the plug flow reactor.

For the experiments on the catalytic influence of carbon dioxide, CO_2 was added to the pure water flow prior to the pre-heater. Gaseous carbon dioxide was taken from the central storage

tank of the Institute and passed to an integrated pump and cooling module, where it was first liquefied and then delivered to a 1 l autoclave at a pressure of 10 to 15 MPa by an air-driven pump. Liquid CO_2 was withdrawn from the autoclave and processed to the reactor by a HPLC pump (Milton Roy miniMetric 1711) at a flow rate of up to 10 ml/min. The actual flow rate was measured by a mass flow meter (Rheonik RHM 015). In order to exclude any disturbances of the metering pumps on the CO_2 flow, a check valve was installed upstream of the mixing point.

The reactor was equipped with two additional heating jackets (2 kW each) in order to compensate for heat losses or to further increase the maximum outlet temperature. Afterwards the reactor effluent was immediately cooled down by passing a double pipe heat exchanger operated with tap water as the cooling medium, thus rapidly terminating the reaction. The effluent subsequently passed a spring-loaded backpressure regulator (IMF-Vatec DV 943/INOX) where it was expanded to ambient pressure. The system pressure could be set by adjusting the load of the spring in the regulator valve. The liquid as well as the gaseous effluents were processed to the effluent collection and measurement system afterwards.

Liquid samples were not taken before a time corresponding to five to ten residence times had passed at steady-state conditions. The effluents were collected in glass flasks and subjected to the respective analytical methods. In order to measure the volumetric gas production as well as the product gas composition, a burette system combined with a sampling vessel was installed. At the beginning of the gas measurement the effluents were passed in an upward direction through the glass vessel (V = 25 ml). This procedure led to the displacement of any air initially present. Afterwards the cylinder was rotated into a horizontal position and gas produced in the course of the reaction was trapped in the upper part of the shell. Gas samples could be taken through a septum with a gas tight syringe (Hamilton gas tight, V = 1000 µl) and were immediately injected into a gas chromatograph for composition analyses. The total volume of the effluents entering the system within a certain time could be determined by reading the difference in the liquid level in the burette. The burette system was connected to a compensator reservoir with adjustable vertical position in order to equalize the pressure within the system to ambient pressure.

In order to minimize pressure fluctuations, which were due to the operation of the pumps and the pressure regulator, the system was connected to a buffer vessel, which had an internal volume of 3.5 l and was filled with a compressible nitrogen headspace.

The pre-heaters and the reaction pipes were electrically heated by means of 5 heating jackets, which could be adjusted separately by a temperature control system (Horst HT-60 controller). In order to decrease the heat losses to the surroundings, the complete high temperature section of the apparatus was thermally insulated.

The system pressure was measured by a pressure transducer. Temperatures at the outlet of the pre-heaters as well as at the inlet and the outlet of the reactor were measured with high temperature resistant NiCrNi-thermocouples, which were inserted into the reaction pipes by

means of tee-connectors. Both pressure and temperatures were constantly measured and recorded by a data acquisition system. The aqueous flow through the reactor was measured gravimetrically by weighing the feed and the sample vessels with laboratory scales, since mass flow meters, which are based on the Coriolis-principle, bear the risk of clogging when suspensions containing larger particles are discharged through their internal tubes.

3.2.2 MODIFICATIONS TO SET-UP FOR CONTINUOUS WATER OXIDATION

For the continuous water oxidation of lignocellulosic biomass, the set-up described above was partially modified. Due to the corrosive atmosphere of high-temperature water in the presence of an oxidant, a new reaction coil made of corrosion-resistant nickel alloy (Inconel, Alloy 600, OD 6.35 mm, ID 2.13 mm) with an internal volume of 20 ml was installed downstream of the mixing point. This reactor could either be connected to the existing reaction coils, in order to extend the residence time and increase the outlet temperature under hydrolytic conditions, or it could be used as a replacement for the existing coils in continuous water oxidation. In the latter case, the reaction coil was directly connected to the mixing point by Inconel pipes and fittings. The reactor was placed in a 4 kW oven (Heraeus RO 7/75), which in principle allows for temperatures up to 1000°C. Under operating conditions, reactor outlet temperatures up to 500°C could be accomplished.
Hydrogen peroxide was used as the oxidant. It was directly introduced into the feed vessel and delivered to the reactor along with the biomass in order to facilitate the experimental procedure.

3.2.3 FIXED BED ASSEMBLY FOR SEMI-CONTINUOUS OPERATION

In some experiments, the reaction coils were replaced by a fixed bed assembly as an alternative means to extend the residence time of solid particulates within the reaction zone. The principle of this set-up is illustrated in Figure 3.2.

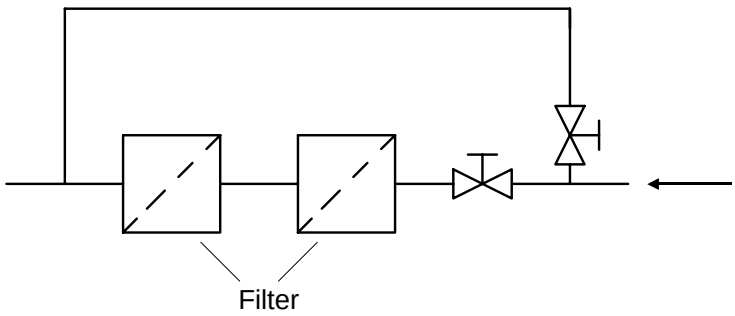

Figure 3.2: Fixed bed assembly for the semi-continuous treatment of biopolymers

The fixed bed was made of two T-filter (Swagelok, model SS-4TF-05) units which were coupled by a piece of high pressure piping. The solid material, e.g. wheat straw and organosolv lignin, was filled in the sinter metal inlet of the upstream unit and was contained between the filters during the experiment. About 0.5 g of solid material could be retained between the filter units. In order to minimize the time required for heating up the assembly to operating temperatures, a bypass was added to the system. During the heating up period pure water was processed through the bypass to avoid the onset of any reactions within the fixed bed. Once the desired temperature was reached, the high temperature valves (Sitec, model 710.5315) were switched and the water stream was allowed to flow through the fixed bed containing the biomass for a preset time period. At the end of this holding time, the second metering pump was turned on to introduce cold water and to rapidly decrease the temperature in the fixed bed. Due to the significant heat capacity of the body of the valve and the filter units, a marked temperature fall could be observed during the first minutes, followed by a temperature increase to the desired level.

3.3 Analytical methods

Different analytical methods were used to characterize the effluents of the hydrothermal treatment. The dissolved organic carbon (DOC), total organic carbon (TOC), total nitrogen (TN) as well as the chemical oxygen demand (COD), ammonia nitrogen (NH_4-N) and nitrate (NO_3-N) were measured to calculate the respective carbon and nitrogen balances. Beside the determination of these lumped parameters, several GC and HPLC methods were employed in order to provide a more detailed insight into the product formation and to identify and quantify main degradation products. The analytical approaches for the different classes of compounds are described in the following.

3.3.1 DETERMINATION OF SUM PARAMETERS

The input materials were characterized with respect to their dry matter content and their elementary composition in terms of carbon, nitrogen, and sulphur. The dry matter content was measured by filling samples in evaporation bowls and subsequent drying in a desiccator cabinet at 105°C. The water content of the material was determined by measuring the weight loss of the samples after a drying period of 48 h. The elementary composition of solid matter was determined in the Central Analytical Laboratory of Technische Universität Hamburg-Harburg by burning samples in a CNS-analyser (Leco-2000-CNS-Analyser) at temperatures from 1000 to 1450°C. The amounts of carbon and sulphur were measured by analysing the concentration of the respective oxidised compounds (CO_2, SO_2) with infrared detectors in the off-gas. The concentration of nitrogen was measured by means of a heat conductivity detector.

Effluents of the hydrothermal degradation of biomass were analysed for their carbon and nitrogen content with fully automated analysers in the Central Analytical Laboratory (Elementar HighTOC + TNb) and at the Institute of Bioprocess and Biochemical Engineering (Multi N/C 3000). For the determination of the dissolved organic carbon (DOC), effluent samples were passed through a 0.45 µm filter prior to injection, in order to retain suspended particles. The samples were first acidified by phosphoric acid to remove any inorganic carbon and afterwards subjected to catalytic incineration. With the instrument available at the Central Laboratory, finely suspended particles could also be injected. Provided that the effluent suspensions had a low concentration of insoluble matter, the total organic carbon (TOC), being the sum of dissolved carbon and insoluble carbon, could thus be determined.

The quantification of chemical oxygen demand (COD), ammonia nitrogen (NH_4-N), and nitrogen in form of nitrate (NO_3-N) was accomplished by using standardized photometric test kits (Dr. Lange).

3.3.2 SACCHARIDE ANALYSIS

Sugar analyses were conducted by means of HPLC with a ligand exchange chromatography (LEC) column in the Central Analytical Laboratory of Technische Universität Hamburg-Harburg. The technical specifications and the operating conditions of this system are stated in Table 3.2.

Table 3.2: Specifications of the HPLC system for the analysis of saccharides

Technical Specifications	HPLC	Macherey Nagel, Nucleogel®Sugar
	Column Type	Packed Column; L = 300 mm, ID = 7.8 mm Packing material: Cation exchange polymer
	Guard Column Type	Packed Column; L = 21 mm, ID = 4 mm
	Detector Type	Refractive Index
Operating Conditions	Eluent	Distilled Water
	Eluent Flow	0.5 ml/min
	Oven Temperature	72°C, isothermal

Pure demineralized and degasified water served as the eluent and was delivered with a piston pump (Merck-Hitachi-L7100) at a flow rate of 0.5 ml/min into a 6 way injection valve (Rheodyne 7725i). Product samples were first centrifuged at 13000 rpm to remove solid impurities. Subsequently the supernatant was passed through a filter unit (0.2 µm) prior to injection. A guard column was installed upstream of the separation column to remove further impurities, e.g. salts and peptides. Small amounts of the liquid samples were injected (injection

volume 20 µl) into the eluent flow and separated with a Nucleogel®Sugar column packed with a cation exchange polymer. This packing material is especially designed to separate mono- and disaccharides and the degradation products thereof. The components were identified with a refractive index detector (RI-IV LCD Analytical). Peak identification and quantification of the components detected with this system were accomplished by injecting standard solutions with known composition at different concentrations, in this way allowing to convert peak areas to concentration values. All samples were analysed in triplicate for reasons of reproducibility.

3.3.3 ANALYSIS OF CARBOXYLIC ACIDS

Carboxylic acids, especially acetic acid, are known to be refractory compounds [39] which are formed in larger quantities during hydrothermal treatment and have a major contribution to the residual DOC after oxidation [40]. Reaction effluents were therefore analysed for carboxylic acids with the system specified in Table 3.3.

Table 3.3: Specifications of the GC system for the analysis of carboxylic acids

Technical Specifications	Gas Chromatograph	Varian 3900
	Column Type	WCOT FUSED SILICA (25 m, ID = 0.32 mm, Coating: FFAP-CD, DF = 0.3 µm)
	Detector Type	Flame Ionisation Detector FID
Operating Conditions	Carrier Gas	Nitrogen
	Carrier Flow	1 ml/min
	Split Ratio	0 – 1 min splitless, 1 – 2 min: 1/100, after 2 min: 1/20
	Injector Temperature	220 °C
	Oven Temperature	60 °C (1 min) – 10 °C/min until 200 °C 200 °C (2 min)
	Detector Temperature	230 °C
	Injection Volume	0.5 µl

The system consisted of a gas chromatograph (Varian 3900) equipped with a capillary column (WCOT fused silica) and a flame ionisation detector operated at 220°C. The samples were acidified by 2 % phosphoric acid prior to injection. For each run a sample volume of 0.5 µl was injected using nitrogen as carrier gas. The temperature program was as follows: After an initial holding time of 1 min at 60°C the oven temperature was increased by a rate of 10°C/min to the final temperature of 200°C. By this method carboxylic acids higher than formic acid can be detected and quantified. Formic acid cannot be detected by FID but would require alternative methods like HPLC for detection.

3.3.4 GC-MS ANALYSIS OF DEGRADATION PRODUCTS

GC-MS analyses were run on selected effluents of the hydrothermal treatment of lignin, wheat straw, and naphthalene to identify and quantify main degradation products. The analyses were conducted at the Central Analytical Laboratory of Technische Universität Hamburg-Harburg according to the method described in Table 3.4.

Table 3.4: Specifications of the GC-MS system for the identification and quantification of products

Technical Specifications	Gas Chromatograph	Hewlett-Packard 5890 II
	Column Type	DB-5ms (30 m, ID = 0.25 mm, DF = 0.25 µm)
	Detector Type	MSD 5971A
Operating Conditions	Carrier Gas	Helium 5.5
	Column Pressure	65 kPa
	Split Ratio	Splitless
	Solvent	Dichloromethane
	Injector Temperature	300 °C
	Oven Temperature	70 °C (2min) – 5 °C/min (170°C) – 10 °C/min (290 °C) – 290 °C (10 – 15 min)
	Interface Temperature	280 °C
	Ionisation	EI (70 eV)
	Detector Temperature	182 °C
	Injection Volume	2 – 4 µl

The system used for the analyses was a HP5890 gas chromatograph with a HP5971A MS engine. The ionisation was accomplished by EI (70eV). A two-step temperature program was applied for separating the reaction products on a capillary column (DB-5ms): Starting temperature: 70°C (2 min) with a subsequent heating rate of 5°C/min to 170°C and a following heating rate of 10°C/min to 290°C and a final holding time of 10-15 min at 290°C. An aqueous sample of 4 ml was extracted with an equivalent volume of dichloromethane.

3.3.5 NAPHTHALENE ANALYSIS

The residual amount of naphthalene in the reaction effluents was determined quantitatively at the Institute for Thermal and Separation processes. After a single-stage extraction of 2 ml of effluent with an equivalent volume of toluene, the samples were subjected to the GC method described in Table 3.5.

Table 3.5: Specifications of the GC system for the quantification of naphthalene

Technical Specifications	Gas Chromatograph	Hewlett-Packard 5890
	Column Type	J & W DB5 (30 m, ID = 0.25 mm , DF = 0.1 µm
	Detector Type	Flame Ionisation Detector FID
Operating Conditions	Carrier Gas	Nitrogen
	Column Pressure	75 kPa
	Split Ratio	1/50
	Solvent	Toluene
	Injector Temperature	300 °C
	Oven Temperature	100 °C (2 min) – 10 °C/min until 320 °C 320 °C (7min)
	Detector Temperature	350 °C
	Injection Volume	1 µl

Pure naphthalene was extracted with toluene and injected into the chromatograph for the determination of the retention time. The quantification was accomplished by means of a calibration curve applying different naphthalene concentrations and evaluating the respective peak areas.

3.3.6 AMINO ACID ANALYSIS

The separation and detection of amino acids was accomplished by a RP-HPLC-system with derivatization of the amino acids prior to separation and fluorescence detection of the derivatives. The main specifications for this system are summarized in Table 3.6.

Table 3.6: Specifications of the HPLC system for the analysis of amino acids

Technical Specifications	HPLC	Merck, Superspher 4 RP18
	Column Type	Packed Column; L = 250 mm, ID = 4 mm
	Detector	Fluorescence, 340/420nm
Operating Conditions	Eluent	A: Sodium acetate; B: Methanol
	Eluent Flow	0.7 ml/min
	Eluent Mode	Isocratic, Gradient
	Oven Temperature	40°C, Isothermal

The effluents were treated with borate buffer and protein precipitant and were centrifuged at 16.000g. Afterwards the derivatization was performed with ortho-Phtaldialdehyde (OPA) and 15µl of the resulting reaction mixture were injected into the column.

Peak identification and quantification of the amino acids were accomplished by injecting external standards with known concentration of the amino acids. By injecting β-Alanin, which does not belong to the group of proteinogenic amino acids, as an internal standard, the peak area ratio of sample and standard solution could be determined, thus allowing to determine the amino acids concentration very accurately. This method is capable of detecting and quantifying all proteinogenic amino acids.

3.3.7 GAS PHASE ANALYSIS

For selected experimental runs, the off-gas of the hydrothermal treatment was characterized in terms of composition and volumetric flow rate. The composition of the gas phase was analyzed with a gas chromatograph (model Perkin Elmer 8500) equipped with a heat conductivity detector (HCD). Gas samples were taken from a gas mouse with a gas tight syringe and were immediately injected in the GC operated in off-line mode. The technical details of the gas chromatograph are depicted in Table 3.7.

Table 3.7: Technical specifications and mode of operation of GC analysis for gas phase measurements

Technical Specifications	Gas Chromatograph	Perkin Elmer 8500
	Column Type	Packed Column; L = 2m, ID = 2mm Packing: Propak Q 100-120 mesh
	Detector Type	Heat Conductivity Detector
Operating Conditions	Carrier Gas	Helium 4.6
	Carrier Flow	15 ml/min
	Oven Temperature	120°C, isothermal
	Injector Temperature	120°C
	Detector Temperature	120°C
	Injection Volume	400 µl

Helium (purchased from Westfalen AG) was chosen as the carrier gas since its thermal conductivity is distinctly different from those of most other gaseous components under the operating conditions stated above, thus allowing the identification of main constituents like carbon dioxide, nitrogen, and methane. Peak identification was accomplished by injecting

standard samples of the pure components and measuring their retention times. The quantitative analysis of the effluent gas composition was done according to the area percentage method, which leads to the determination of the quantitative ratio of the components instead of absolute concentration values.

4 EXPERIMENTS ON MODEL COMPOUNDS

Isolated cellulose and lignin were selected as model compounds for real lignocellulosic biomass, since they are the main constituents of plant biomass beside polyose (hemicellulose). Cellulose and lignin amount to approximately 50 % and 25 % of woody biomass, respectively. Polyose was not treated separately in this work, since it is known to be much more readily degradable due to its less crystalline structure than cellulose and its lower degree of cross-linking compared to lignin.

The main objective of the work with model compounds was to gain information about the achievable degree of liquefaction and about main degradation products. It was further intended to develop a suitable model for the description of the liquefaction kinetics and the kinetics of product formation. In case of cellulose, the acidification by adding carbon dioxide was studied as a supplementary technique to enhance the rate of hydrolysis. Lignin was treated at both hydrolytic and oxidative conditions by applying hydrogen peroxide. The oxidation of lignin was conducted to show the feasibility of a complete removal of any insoluble carbon of lignocellulosic biomass. In addition, the partial oxidation of lignin was studied with respect to the formation of valuable degradation products.

4.1 Liquefaction of cellulose

A systematic study of the liquefaction of pure cellulose in subcritical and near-critical water was conducted for two reasons. Firstly, cellulose is the most abundant biopolymer in the world and the most important constituent of plant derived biomass. Cellulose accounts for the main part of the fibre fraction of the waste specified by ESA, so that it can be considered as a proper model compound for the conversion of plant biomass. Secondly, cellulose was employed to elucidate the feasibility of enhancing the conversion to water-soluble products by adding carbon dioxide. By this means the pH can be lowered and acid-catalysed reactions will presumably proceed at faster reaction rates. The acid-catalysed pathway of cellulose hydrolysis is illustrated in Figure 4.1.

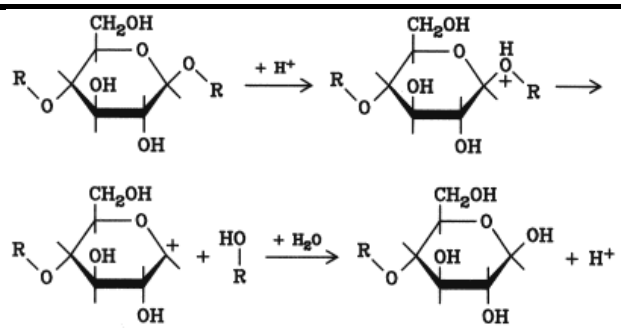

Figure 4.1: Reaction scheme of the acid-catalysed pathway of cellulose hydrolysis

The main objective was the conversion of cellulose to water-soluble degradation products. Therefore, a detailed parameter study on the continuous liquefaction of cellulose was conducted, covering temperatures from 240 to 374°C at residence times in the order of a few seconds to three minutes and initial cellulose concentrations of 0.5 to 1 wt-%. Carbon dioxide was added at different concentrations with respect to saturation in order to investigate the influence of acidification by carbonic acid on the degradation behaviour.

Based on the experimental studies, a kinetic description of the cellulose degradation and the formation of main degradation products was accomplished.

4.1.1 KINETICS OF CELLULOSE DEGRADATION

Discussion of results on cellulose liquefaction:

Continuous experiments on the liquefaction of pure cellulose were conducted with an initial cellulose concentration of 0.5-1 wt-% in the feed suspension, which yielded a cellulose concentration of 0.1-1 wt-% at the reactor inlet, depending on the mass flow ratios of feed and pure water flux. For this diluted system the reaction kinetics were assumed to be independent of the solid concentration and the evaluation in terms of residence time was performed using the properties of pure water [41].

The degree of liquefaction was calculated as the conversion of insoluble carbon to soluble carbon. Assuming that cellulose exhibits a negligible solubility in water, which was confirmed by own measurements, the degree of liquefaction on a carbon basis can be written as follows:

$$f = \frac{DOC_{out}}{TOC_{in}} \qquad (4.1)$$

with DOC_{out} denoting the soluble carbon at the outlet and TOC_{in} the insoluble carbon at the inlet of the flow reactor. The degree of liquefaction equals the degree of cellulose conversion **in case of negligible gas formation**.

The dissolved organic carbon content of the effluent was determined analytically by DOC measurement. The total organic carbon at the inlet of the reactor was calculated on the basis of the amount of cellulose and the cellulose composition. For this purpose, the theoretical portion of carbon in pure cellulose (44.4 wt-%) was corrected for a factor of 0.98 in order to account for impurities. In addition, the dry matter content of cellulose was measured as 95 %, such that the concentration of carbon in cellulose was taken as 41.4 wt-% for calculations.

The degree of liquefaction versus time at temperatures from 240 to 260°C is depicted in Figure 4.2.

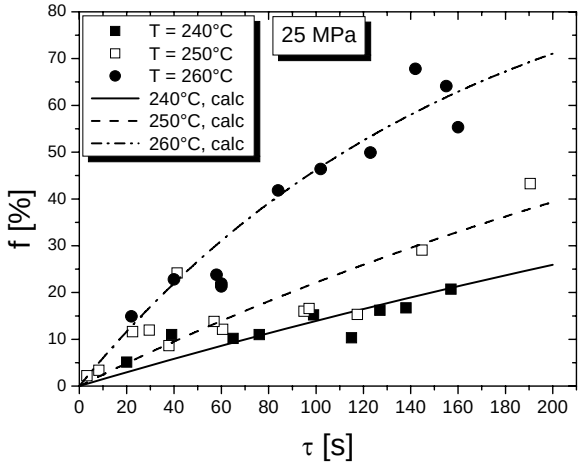

Figure 4.2: Degree of liquefaction of cellulose on a carbon basis at 240-260°C, initial cellulose concentration: 0.5 wt-%, the kinetics were calculated according to a first order approach

It can be inferred that the degree of liquefaction increases with temperature and reaction time. Cellulose is substantially liquefied at a temperature of 240°C, yielding degrees of liquefaction of about 20 % at a residence time of three minutes. A further extension of residence time was not possible because of technical limitations with respect to the available reactor volume and the feasible flow rates.

The degree of liquefaction progressively increases with temperature. At 260°C, about 60 % of the influent carbon were liquefied at a reaction time of 160 s. The experimental data reveal a still increasing tendency of liquefaction at the conditions applied. In order to study the feasibility of a complete liquefaction of any carbon, additional experiments were conducted in the same time range but at higher temperatures. The results of cellulose hydrolysis at temperatures of 270°C and 280°C are shown in Figure 4.3

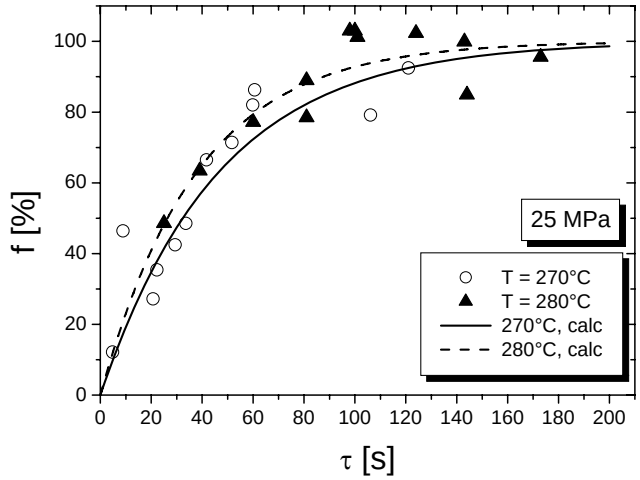

Figure 4.3: Degree of liquefaction of cellulose on a carbon basis at 270-280°C, initial cellulose concentration: 0.5 wt-%, the kinetics were calculated according to a first order approach

As compared to the results before, the cellulose degradation is strongly enhanced by a further increase in temperature. At a temperature of 280°C, essentially all carbon is liquefied at reaction times of 100-120 s. These results prove that pure cellulose can be efficiently degraded to water-soluble products by hydrolysis in water at elevated temperatures and pressures. A further increase in temperature led to even more rapid degradation kinetics, as illustrated by the results of experiments at 290°C and 310°C shown in Figure 4.4.

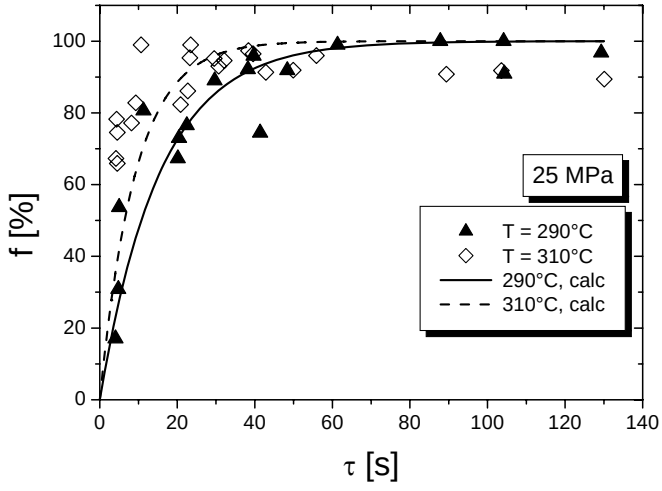

Figure 4.4: Degree of liquefaction of cellulose on a carbon basis at 290-310°C, initial cellulose concentration: 0.5 wt-%, the kinetics were calculated according to a first order approach

At a temperature of 290°C, a complete liquefaction could be achieved within residence times of 60 to 80 s, while at 310°C a complete conversion to soluble products was accomplished after 20 to 30 s. Although the rate of liquefaction initially was further enhanced by a temperature increase, the degree of liquefaction seems to decline with prolonging reaction time at 310°C. This observation can be attributed to different possible explanations, e.g. experimental uncertainties, formation of product gases, and secondary reactions to insoluble products. Experimental uncertainties as a reason for this observation are unlikely. The plausibility of the experiments was checked by calculation of the respective carbon balances. In addition, blank tests on the continuous processing of cellulose at ambient temperature were conducted. A comparison of the expected and the real cellulose concentration in the effluents did not reveal significant deviations, which might have been due to sedimentation and accumulation of insoluble matter in the apparatus.

Cellulose and primary reaction products are known to further decompose to gaseous products in sub- and supercritical water [42]. The gasification of glucose to yield carbon dioxide, hydrogen, and methane is illustrated in Figure 4.5.

$$C_6H_{12}O_6 + 6H_2O \rightarrow 6CO_2 + 12H_2$$

$$C_6H_{12}O_6 \rightarrow 3CH_4 + 3CO_2$$

Figure 4.5: Reaction schemes of glucose gasification in sub- and supercritical water

The formation of methane is the preferred reaction pathway at lower temperatures, while the production of hydrogen proceeds in the supercritical region. A substantial conversion to gas species is, however, usually accomplished at much higher temperatures (400-500°C) and residence times in the order of hours. This finding could be supported by own gas measurements at temperatures of 350 to 375°C and residence times from 20 to 40 s, which yielded a contribution of gas species to the carbon balance of about 1 wt-%. A marked gasification of cellulose can therefore be excluded at the conditions applied.

The decrease in liquefaction at higher temperatures and prolonged residence times is presumably due to the formation of insoluble products. Such compounds could be formed because of secondary or competing, free-radical reactions. This assumption was supported by visual observations. Effluents, which were treated at temperatures exceeding 300°C, showed precipitation of fine, brownish particulates after a short time at room temperature.

In contrast to temperature, the operating pressure had a negligible influence on cellulose degradation at the conditions applied. The hydrolysis of cellulose was studied for three different pressure levels at 15 MPa, 20 MPa, and 25 MPa, and temperatures of 250°C and 290°C. The results for 290°C are depicted in Figure 4.6.

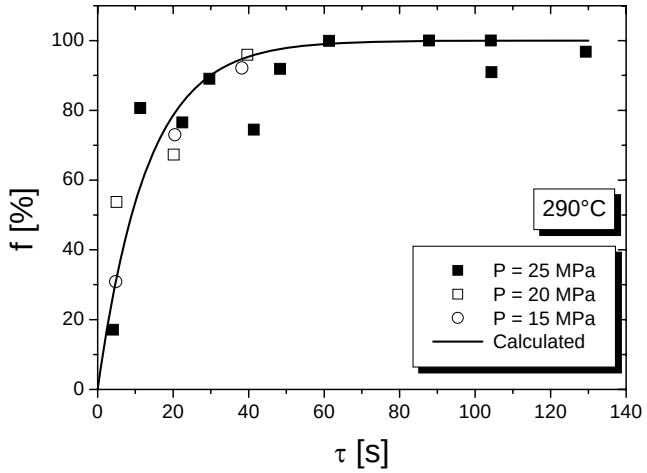

Figure 4.6: Influence of pressure on the degree of cellulose liquefaction, initial cellulose concentration: 0.5 wt-%

As can be seen, a marked influence of pressure cannot be distinguished at a temperature of 290°C. This result can be explained by the fact, that water still has the character of an incompressible fluid even at temperatures in the range of 300°C. The density of pure water at 300°C [41] changes from 742.9 kg/m^3 at 25 MPa, to 734.8 kg/m^3 at 20 MPa, and 725.7 kg/m^3 at 15 MPa, which corresponds to a weak decrease in density of 1.1 % and 2.3 %, respectively. Accordingly, physico-chemical properties associated with density, e.g. the dielectric constant, dissociation and reaction constants, do not change significantly with pressure.

In order to assess the plausibility of the results, a mass balance check was performed for a larger number of experiments. For this purpose, the total organic carbon of the effluent, being the sum of dissolved and insoluble carbon in the liquid phase, was measured by TOC analysis. The measured values were compared to the calculated influent carbon to elucidate whether the carbon balance was fulfilled. The calculation for 50 experiments yields a mean relative deviation of 9.5 % with respect to influent and effluent carbon. The values fluctuate arbitrarily rather than showing a clear tendency towards a higher or lower effluent carbon content as compared to the calculated influent carbon. This deviation might well be due to inaccuracies in the TOC analysis itself and not necessarily to experimental errors, since the injection of solid-bearing suspensions into the TOC-analyser could not be accomplished as reproducibly as the analysis of filtrated samples.

Due to the high density of data points, not every single experiment could be repeated in duplicate or triplicate. The reproducibility of experiments was checked by means of selected experiments, representing typical operating conditions. Experiments at 240°C and 120 s, 260°C and 160 s, as well as 280°C and 80 s were done in duplicate. In addition, an experiment at 260°C and 60 s was repeated in triplicate. The degrees of conversion and the relative

deviation from the respective mean values were calculated and averaged over all experiments. The resulting mean relative deviation was 6.6 %, which is satisfactory taking into account that the analysis of effluents was also afflicted with uncertainties.

Kinetic modelling:

The experimental data on the liquefaction of pure cellulose were modelled using a global rate law, with the reaction order of cellulose being unity. For such an irreversible first order reaction, the rate of reaction can be expressed as follows:

$$r = -kC_0(1-f) \qquad (4.2)$$

with k denoting the reaction rate constant and C_0 being the initial cellulose concentration. For modelling the degree of liquefaction by the concept of an ideal plug flow reactor, the following assumptions are made [43]:

- isothermal conditions
- plug flow in axial direction
- no gradients in radial direction (temperature, pressure, concentration)
- no axial dispersion

The assumption of isothermal conditions is justified because of the negligible temperature difference between the reactor inlet and outlet. The experiments were conducted at high axial velocities, with typical Reynolds numbers in the range of 3,000 to 8,000. It can therefore be assumed that axial diffusion is negligible compared to convection and that the turbulent regime accounts for plug flow and negligible radial gradients.

Due to the low compressibility of water and the low cellulose concentration , the fluid density can be assumed as constant along the reactor. At these conditions, the degree of cellulose liquefaction in an ideal plug flow reactor can be expressed as follows:

$$f = 1 - \exp(-k \cdot \tau) \qquad (4.3)$$

and after rearrangement:

$$-\ln(1-f) = k \cdot \tau \qquad (4.4)$$

In case the rate of conversion can accurately be described by a first order kinetic, the reaction rate constant can be read as the slope of a straight line in a ln(1-f) versus τ diagram. Such a diagram is depicted in Figure 4.7 for the temperature range from 240 to 310°C.

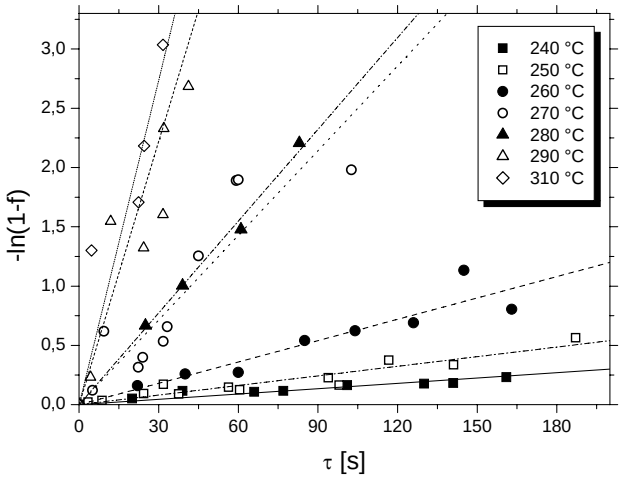

Figure 4.7: Determination of the reaction rate constant from the respective conversion data

As can be seen, the experimental data can reasonably be reflected by straight line relationships. Accordingly, the kinetics of cellulose liquefaction can satisfactorily be described by a global first order rate law. This approach is especially applicable for lower temperatures, where the data very accurately obey a linear relationship.

The reaction rate constants at different temperatures can be determined by reading the values of the slope of the straight lines. These values are stated in Table 4.1.

Table 4.1: Reaction rate constants of cellulose liquefaction at different temperatures

T [°C]	240	250	260	270	280	290	310
k(T) [1/s]	0.0015	0.0025	0.0062	0.0214	0.0263	0.0647	0.1086

A common approach to express the temperature dependence of the reaction rate constant is the Arrhenius' law:

$$k_{(T)} = k_0 \cdot \exp(-\frac{E_{C,A}}{R \cdot T}) \qquad (4.5)$$

with k_0 being the pre-exponential factor and E_A the activation energy of the reaction.

Accordingly, these kinetic parameters can be determined by plotting ln(k(T)) versus the reciprocal temperature and reading the ordinate intercept and the slope of the straight line. The Arrhenius' plot with the respective values of the pre-exponential factor and the activation energy is shown in Figure 4.8.

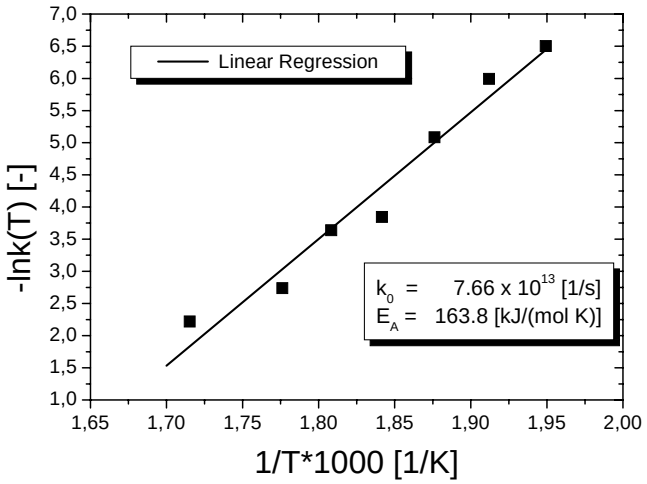

Figure 4.8: Determination of kinetic parameters from the Arrhenius' approach

The straight line was obtained by linear regression of the reaction rate constants at different temperatures. As can be seen, the calculated straight line is in good accordance with the values of the reaction rate constants. Hence, the Arrhenius' law can be applied to the liquefaction of cellulose in subcritical water.

Summing up the results of this parameter study, it can be concluded that the kinetics of cellulose conversion in subcritical water can accurately be described by a global first order rate law.

4.1.2 PRODUCT FORMATION

Beside the kinetics of cellulose hydrolysis, the investigation of product formation was of special interest. The examination of product formation included the identification and the description of temperature and time dependence of main degradation products. A detailed knowledge of product formation is important to optimise reaction conditions with respect to the selective production of desired compounds, e.g. glucose as a valuable product of the hydrolysis of lignocellulosic materials.

The liquid effluents of cellulose hydrolysis were analysed for saccharides and secondary degradation products thereof as well as for carboxylic acids. Figure 4.9 shows a chromatogram of cellulose degradation products.

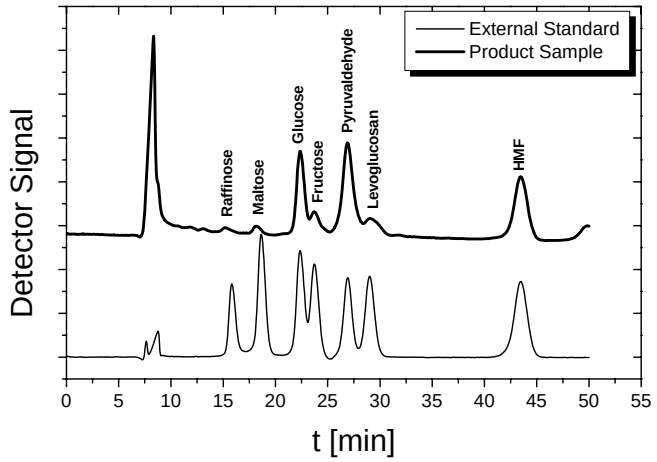

Figure 4.9: Chromatogram of saccharide analysis, experimental conditions: 25 MPa, 290°C, 62 s

It can be inferred that glucose, being the monomeric building block, as well as fructose, which is formed from glucose by isomerization reactions, could be detected in significant amounts. In addition pyruvaldehyde, levoglucosan, and hydroxymethylfurfural (HMF) were formed as secondary reaction products of cellulose hydrolysis. At lower temperatures and residence times, water-soluble oligosaccharides could also be detected as partial hydrolysis products, but not be quantified because of poor peak resolution.

The parameter study showed that glucose, pyruvaldehyde, and HMF are major reaction products of cellulose hydrolysis. These compounds were, however, not stable under operating conditions due to secondary decomposition reactions. The main objective of the studies on product formation was to derive practical conclusions for engineering purposes, e.g. process design and process optimisation, rather than achieving a thorough understanding and modelling of the exact reaction mechanism. Hence, the yields of main degradation products were modelled according to the approach of a simple consecutive reaction. This approach is illustrated in Figure 4.10 considering glucose.

$$\text{Cellulose} \xrightarrow{k_{G,f}} \text{Glucose} \xrightarrow{k_{G,d}} \text{Secondary products}$$

Figure 4.10: Simplified reaction scheme for glucose formation and secondary decomposition

Under the assumption, that both the rate of formation and the rate of decomposition are of first order, the concentration of glucose can be calculated as follows:

$$C_G = \frac{k_f}{k_d - k_f} C_{C,0} \left[\exp(-k_f t) - \exp(-k_d t) \right] \qquad (4.6)$$

with $C_{C,0}$ denoting the initial cellulose concentration and k_f and k_d the rate constants of formation and decomposition, respectively.

The yield of degradation product i on a carbon basis was defined as the ratio of carbon bound in species i to the theoretically possible amount, which was calculated from the initial cellulose concentration.

$$Y_i = \frac{C_i}{TOC} \qquad (4.7)$$

This formula is also valid in case of gas production. The reaction rate constants of formation and decomposition could be determined by fitting equation 4.6 to the experimentally determined yields. Figure 4.11 shows the yield of glucose and HMF as a function of time at 250 to 310°C.

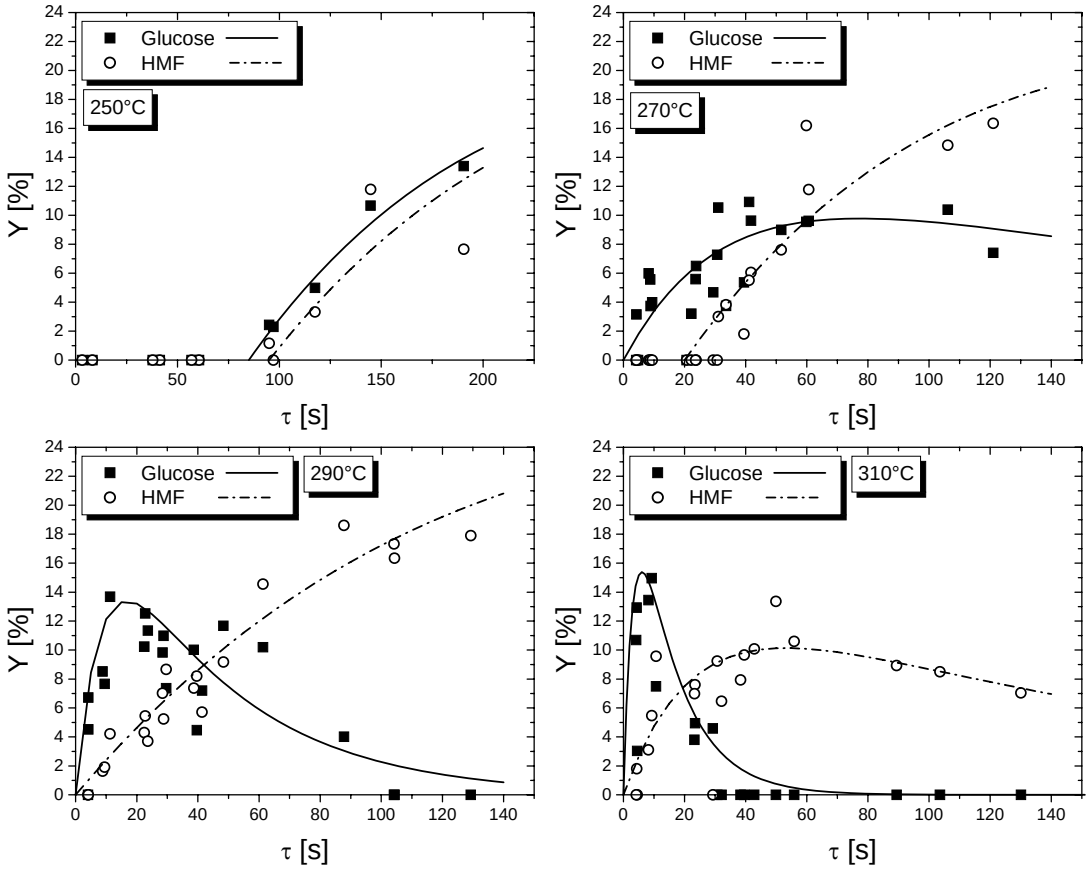

Figure 4.11: Yields of selected degradation products versus time, T: 250-310°C, P: 25 MPa